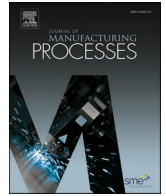




Contents lists available at ScienceDirect

Journal of Manufacturing Processes

journal homepage: www.elsevier.com/locate/manpro

Fabricating plasma bonded microfluidic chips by CO₂ laser machining of PDMS by the application of viscoelastic particle focusing and droplet generation

M. Tahsin Guler*

Department of Physics, Kirikkale University, 71450 Kirikkale, Turkey

UNAM—National Nanotechnology Research Center, Institute of Materials Science and Nanotechnology, Bilkent University, 06800 Ankara, Turkey

ARTICLE INFO

Keywords:

CO₂ laser machining
Microfluidic chip
Plasma bonding
Viscoelastic focusing
Droplet generation

ABSTRACT

In this study, direct CO₂ laser machining of microchannels onto PDMS slabs and plasma bonding for sealing have been shown to provide the fastest method to fabricate PDMS microfluidic chips. Due to resolidification, the ashes and dust remains that cover the PDMS slab surface following this ablation process change the surface chemistry and prevent plasma bonding. Removing these remnants on the surface has been shown to be only possible via attaching and detaching a tape to the surface. The effect of laser frequency, speed and power settings has been investigated over the entire possible range with regards to channel geometry. The best laser settings were determined and the resulting output channels were examined under SEM and optical microscopes. PDMS spin coating after laser machining has been proposed as a pre-treatment process to improve the geometrical features of the channel. Water-in-oil droplet generation in the T-junction, as well as microparticle focusing in viscoelastic fluid – used to sample enrichment – have been shown as examples of applications that benefit from precise direct laser machined microchannels.

1. Introduction

Polydimethylsiloxane (PDMS) is the primary material used to fabricate microfluidic chips because of superior features such as transparency, good bonding to several substrates, biocompatibility, easy casting, easy curing and flexibility. Therefore, the great majority of the environmental components of microfluidic chips, like pumps [1] and valves [2], are PDMS compatible. Nonetheless, the soft lithography technique [3], the gold standard for fabrication of PDMS microchannels, requires cleanrooms that are not available to many researchers. Some alternatively developed techniques remove the need for cleanroom access, like xurography [4], 3D printing [5], micro milling [6] and laser machining [7].

In xurography, first developed by Bartholomeusz et al., [8], a cutter plotter mounted with a razor blade cuts out channels on a spin coated PDMS film, which is then sealed with PDMS slabs from both sides via plasma bonding [4]. This method offers a rapid prototyping of channels down to 100 μm wide and 75 μm deep via an ultra-low cost plotter machine. However, PDMS is very prone to tearing by the razor; in addition, the plotter makes too many errors around the corners, which

limits the use of this method.

Currently, as the most popular rapid prototyping technique, 3D printing offers some solutions for microchannel manufacturing as well. Among the 3D printed microchannel fabrication methods, the one creating PDMS micro channels through casting of a 3D printed mold can achieve channels having a minimum width of 200 μm [9]. While these printers have resolution better than 200 μm, the channel quality falters dramatically in realizing smaller size channels [10]. Because only the stereo lithography or digital light processing-based 3D printers are capable of making molds that are similar to standard microfluidic molds for PDMS casting [11], the 3D printing method is less accessible due to the relatively high cost of the 3D printer devices which have such a feature. In addition, the master mold requires surface treatment in order to peel off the casted PDMS [12], which is an additional complexity with this method.

Mechanical micromachining is also a good alternative for fabrication of PDMS microchannels. A metal working piece is machined with a micro miller to engrave channels on it. Then, the machined metal piece is replicated using a polymeric material. The polymer-based replica is used as a master mold for PDMS casting to form the microfluidic

* Department of Physics, Kirikkale University, 71450 Kirikkale, Turkey.

E-mail address: gulermt@kku.edu.tr.

<https://doi.org/10.1016/j.jmpro.2021.11.016>

Received 20 July 2021; Received in revised form 2 November 2021; Accepted 11 November 2021

Available online 23 November 2021

1526-6125/© 2021 The Society of Manufacturing Engineers. Published by Elsevier Ltd. All rights reserved.

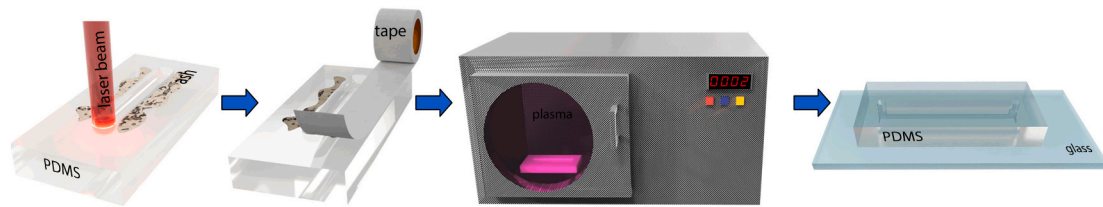


Fig. 1. Illustration of the microchannel fabrication method. CO₂ laser automatically machines the channels directly on the PDMS slab according to the computer aided design (CAD) file and, Ashes and debris are removed from the PDMS surface via a tape to facilitate plasma bonding.

channels [13]. The micro milling enables machining of microchannels down to 100 μm wide and 50 μm high with an affordable CNC milling machine.

Ultra-short pulse lasers, like femtosecond lasers, are capable of engraving many materials including glass [14] and can produce 3D channel geometry in glass [15]. Rather than manufacturing polymer channels, femtosecond lasers are more suitable for machining channels in harder materials like quartz [16], given that the CO₂ laser can already realize polymeric channels in an easier and cost-effective way. It takes 3 h for hydrofluoric acid (HF) etching following laser processing to finish the machining of a microchannel that fits on a standard glass slide [17]; additionally it leaves a very rough surface after etching that needs polishing [18].

Since many different laser sources are available, the parameters used – as well as minimum channel dimensions – vary in the laser machining of PDMS microchannels. Femtosecond laser machining provides a width down to 1 μm for 3D channels [19]. While enabling dimensions as low as soft lithography, femtosecond lasers are very expensive and require complicated optical setups. It also requires further chemical treatment to finish the channel fabrication process, such as running HF flux through the channel following the laser machining to finish the fabrication process. An ultra violet (UV) excimer laser, as a relatively more cost effective option than the femtosecond laser, provides channel widths of around 100 μm by machining a spin coated PDMS layer [20] on a PDMS slab [20]. CO₂ lasers, as cost effective and fully automated devices, are the most suitable type for rapid prototyping purposes that enable channel widths of 100 μm by machining a PDMS layer on an acrylic sheet [21]. In addition, it takes less than 1 min to finish a microchannel that can fit to a glass slide, unlike femtosecond lasers that need a few hours to finish the machining of such a device.

Among other rapid fabrication methods, laser machining comes to forefront within the microfluidic community as a widely adopted method. Giving promising results in thermoplastic engraving [22], CO₂ laser machining has been used to create microfluidic chips for several applications, including on-chip prothrombin time (PT) measurement [23], cytometry [24], droplet generation [25], electrophoresis [26], passive microfluid mixing [27], concentration gradient generators [28], nanofibers [29] and fuel cells [30].

CO₂ laser machining of PDMS is less common than laser machining of thermoplastic materials for microchannel fabrication due to bonding issues. As the photo-ablated material resolidifies over the working piece, the physical and chemical character of the surface is totally changed, and this prevents plasma bonding. One previous study showed laser machining of spin coated PDMS film to make microchannels by suggesting a special range of laser parameters that produce relatively low ashes during the ablation [31], but the plasma bonding performance of the laser-machined PDMS was not shown. Another study that focused on producing microchannels from spin coated PDMS film through double PDMS to PDMS casting carried out laser ablation over the acetate sheet. Reversing the PDMS coated acetate sheet over the glass slide sandwiches the PDMS film, which blocks the ashes covering the PDMS surface and therefore facilitates plasma bonding [21].

PDMS film laser machining produces rectangular profile microchannel the depth of which is regulated through the thickness of the

PDMS film via the spin coating rate. Although being a rapid prototyping method, PDMS film laser machining includes some cumbersome steps such as PDMS spin coating, curing, reversing the PDMS layer over a glass slide, bonding the machined layer to a PDMS slab, and gently peeling off the acetate sheet from the PDMS layer without tearing.

Producing microchannels by laser machining of bulk PDMS slabs has none of these impractical processes such as molding, casting, spin coating etc. So far, a few studies have focused on the direct machining of bulk PDMS with a CO₂ laser. Holle et al. [32] just investigated the effect of laser parameters, power and speed on the channel dimensions and profile. Fogarty et al. [33] optimized the machining parameters to make a capillary electrophoresis microfluidic chip by contact bonding the PDMS to glass. The contact bonding is a reversible sealing method for PDMS microchannels, which works only at very low fluidic pressure, is very vulnerable to the external forces that a microfluidic chip can possibly face. Yuen et al. employed a tacky bonding method, which is a bonding method that uses an uncured PDMS spin coated substrate that is cured after combining the channel and the substrate [34]. This dirty bonding method only creates an all PDMS microfluidic chip since a PDMS substrate is mandatory for sealing the PDMS microchannels. Thus, advantages of using a glass substrate like easy material deposition for fabricating electrodes [35] or MEMS [36], are given up.

This current study provides a complete guide to make a microfluidic chip by direct laser machining of a PDMS slab that takes only 10 min to produce the chip from scratch. Fig. 1 illustrates the general steps of the fabrication procedure of a microfluidic chip with this method. A simple approach to remove the ashes and debris inherited from the ablation process is presented that enables plasma bonding to create high pressure resistant and durable microfluidic chips. Thus, laser ablation, which is the only method providing direct carving of channels onto bulk PDMS, presents the fastest method for fabrication of PDMS microfluidic chips. In addition, this study presents geometric characteristics of the channel top and the channel edge along the laser machining direction, as well as intersections of the channels, in detail. Also, a method to improve the channel surface smoothness is shown, which provides more optical clarity for better visual inspection. Droplet generation and micro particle separation in viscoelastic fluid used can be achieved with the microfluidic chips produced by this method.

2. Materials and methods

2.1. Preparation of materials

PDMS (Sylgard 184, Dow Corning) was prepared in a 1/10 (w/w) ratio with its curing agent by vigorously mixing a total of 30 + 3 g. After degassing the mixture, it was poured onto a 5 inch glass Petri dish and cured at 100 °C for 12 h. Then, it was peeled off the Petri dish by gentle separation.

A solution of 1000 ppm hyaluronic acid (HA) (molecular weight = 1.5 MDa – NewDirections) was prepared by mixing it with a magnetic stirrer at 20 rpm for 2 days. Fifty microliters of 6 μm diameter mono disperse polystyrene (PS) micro beads (Polysciences, Inc.) were added into 2 ml of HA solution and taken into a syringe.

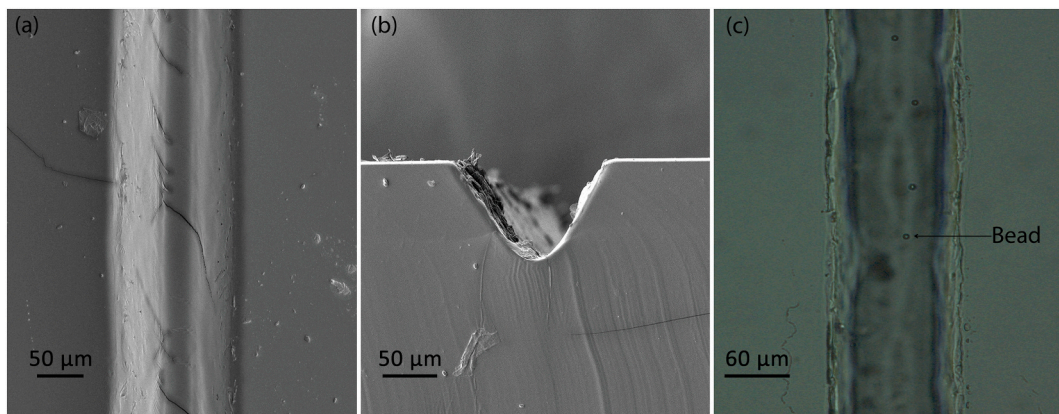


Fig. 2. SEM image from a) top perspective and b) cross section of the laser machined PDMS microchannel at 5 kHz, 14% P and 100% S settings. c) Inverted microscope image of the microchannel filled with 6 μm PS particles suspended in DI water solution.

2.2. Laser machining of the PDMS slab

A CO₂ laser (Epilog Zing 30 W, USA) was used in vector cutting mode to engrave the microchannels onto the PDMS surface. The upper surface of the PDMS slab was machined with the laser, not the one in contact with the glass petri dish during the curing on the hot plate. The laser had a 30 W output power (P) 51 mm focal length with a 27.1 mm/s horizontal and 25.5 mm/s vertical speed (S) of operation configured in percentage units from the user interface i.e. 3 W when the laser power was set to 10%. The power and speed settings are given in percentage units throughout the remainder of this study. In addition, the frequency (f) range was between 10 and 5000 Hz. The pulse duration of the laser was shown to be $f^{-1} \times P$ [27] where f was the frequency and P the power. The focal point of the laser was set via the lever hanging over the mobile head carrying the laser focus lens. While the laser had its own function for the up-down motion of the platform, it was not used for arranging the defocusing ratio for two reasons: one was that it was not controlled quantitatively, and the other was that once it was used, the x-y position was lost. Therefore, for defocusing the laser, a small lever jack was placed on the laser platform and the working piece was put over the lever jack, which was moved towards the focus lens by lifting the lever jack up.

2.3. Cleaning

After laser machining of the channels, the PDMS slabs were cleaned using two methods: one was by sonication in an acetone bath, which is a 10-minute process that was followed by washing with DI (deionized) water and baking on a hot plate for 1 min at 100 °C. The other was by attaching and detaching tape (Scotch Crystal 610, 3M) to and from the surface of the slab to lift the ashes and debris from around the channels. The findings show that tape cleaning outperformed the solvent cleaning method. Also, a mini rotary brush (Dremel) was employed to clean the PDMS surface after laser machining.

2.4. Spin coating of PDMS

The PDMS was spin coated on the machined PDMS slab at 5000 rpm for 2 min at an acceleration rate of 2000 rpm/s. The spin coating, which was aimed at removing the surface roughness of the channels, was performed following the optional cleaning. After the spin coating process, the laser machined PDMS slab was left on the hot plate to be cured at 100 °C for 2 h.

2.5. Microscopy

SEM images were obtained after the samples were coated with 10 nm

of gold. The fractures imaged on the objects by SEM were due to cracking of the gold layer formed over the soft PDMS. Inverted microscope images were produced by a Zeiss Axio microscope mounted with its original camera or a high speed camera (Phantom Miro e2). Stereo microscope images were obtained with a cell phone camera (Xiaomi Redmi Note 5) through a binocular microscope (Kruss).

2.6. High speed camera and image processing

A high-speed camera was fitted to the inverted microscope and run at 300 or 7104 frames per second (fps) sampling rates to investigate the viscoelastic particle focusing at low and high flow rates. The recorded video file was investigated with a custom written Python code mainly using the OpenCV library. Using background subtraction, which was followed by some other image processing techniques to track particles and reduce the noise, lateral particle positions and stacked images of particle trains were obtained.

2.7. Simulation

Finite element model (FEM) simulations were performed using COMSOL at normal mesh settings. The channel inlet was configured with a fully developed flow at a constant rate of 6 $\mu\text{l}/\text{min}$, while the outlet was configured with 0 atm constant pressure conditions. The simulation noise was determined via an imaginary particle sweep [37] by measuring the pressure fluctuations of a point inside the channel that gave 0.7% uncertainty to the results of the calculations.

3. Results and discussions

As the laser has a Gaussian beam profile, the channel machined by the laser on the PDMS slab had a Gaussian shape as well.

3.1. The effect of machining parameters on channel quality

Two hundred and fifty-two combinations of different power, frequency and speed settings – scanning the entire range of possible values for each parameter – were tested to analyze the machining quality. The outputs were evaluated in terms of the interior smoothness of the channel, whether to have a straight channel edge, or straight top, etc. According to Table 1S, which gives the results of the test, it was impossible to fabricate a smooth surface microchannel in the low frequency region. The machined channels lacked either a straight channel edge or top in this region. Fig. 1S shows all the kind of outputs achieved by the laser machining of microchannels on PDMS that went towards the generation of Table 1S.

The laser cutter performed perfectly straight channels in terms of

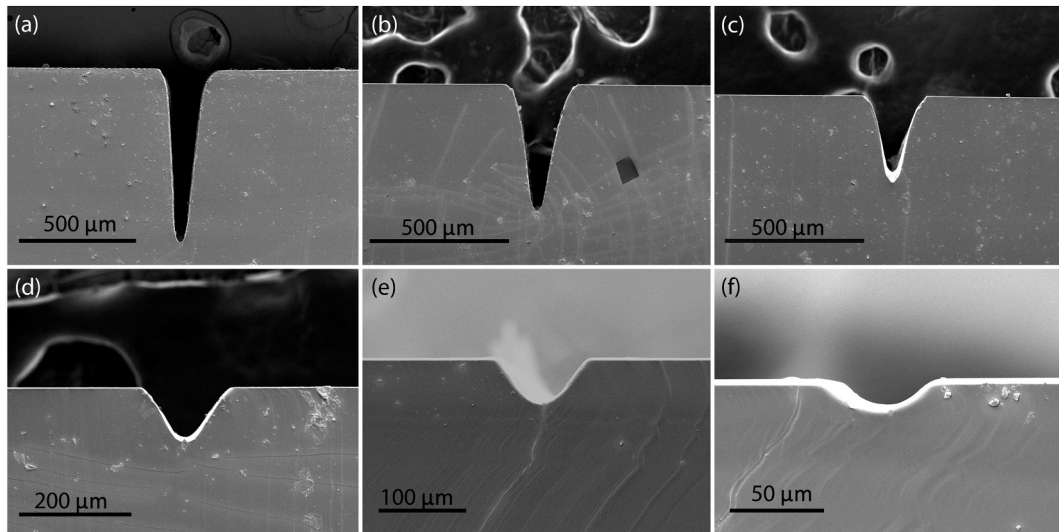


Fig. 3. SEM photo of the cross section of the channels machined at 100% speed, 5 kHz frequency, and a) 100% power b) 75% power c) 50% power d) 20% power e) 15% power and f) 12% power settings.

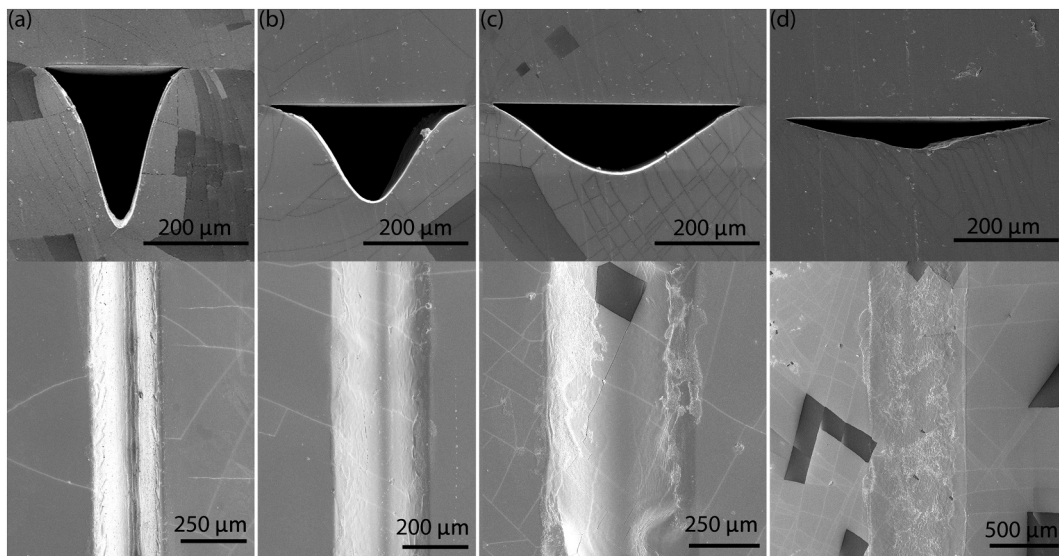


Fig. 4. SEM picture of channels machined with a defocused laser beam at 5 kHz, 100% speed, and 60% power settings. Cross sectional top view outputs are shown for several defocused rates: a) 1.5 mm b) 3 mm c) 4.5 mm d) 6 mm.

smoothness and geometry at the highest frequency region. The best channels that have the smoothest channel surface were achieved at the highest frequency as well as the highest speed settings. The height and width of the channel can be tuned by adjusting the power while using the highest frequency and speed values. Fig. 2(a) shows the smoothness of the channel interior using the SEM image as well as the channel cross section in Fig. 2(b). Fig. 2(c) shows the inverted microscope image of PS microbeads suspended in DI water during the flow through the channel. Therefore, microchannel machining used the highest speed and frequency, as well as low power settings to provide high quality channels allowing precise visual inspection.

3.2. Tuning the channel dimension through the machining parameters

3.2.1. Power

Channel width and height depends on the total laser energy that is transferred to the PDMS working piece, which is proportional to the power and inversely proportional to the speed. Here, the width and

height of the channels that are given in Fig. 2S were machined at the favored setting regimes, which were the highest speed and frequency at several power rates. Fig. 3 shows the SEM image of the machined channels from a cross-sectional viewpoint. Also, the flow velocity profile of water was calculated in COMSOL for several sized microchannels that are given in Fig. 3S. Results showed that the channels engraved at lower than 20% power rate were useful for conventional microfluidic applications, whereas at higher power rates the channel cross section became sharper. Fig. 4S shows the outputs from the top perspective introducing the channel surface features. At higher power rates, the channel lost smoothness becoming rougher while the opposite occurred at lower power rates, which is another point in favor of low-power machining.

The results show that lowering the laser power decreased the curvature of the channel which enhanced the operability with regards to general microfluidic applications.

3.2.2. Defocusing

Laser machining was carried out by putting a working piece on the

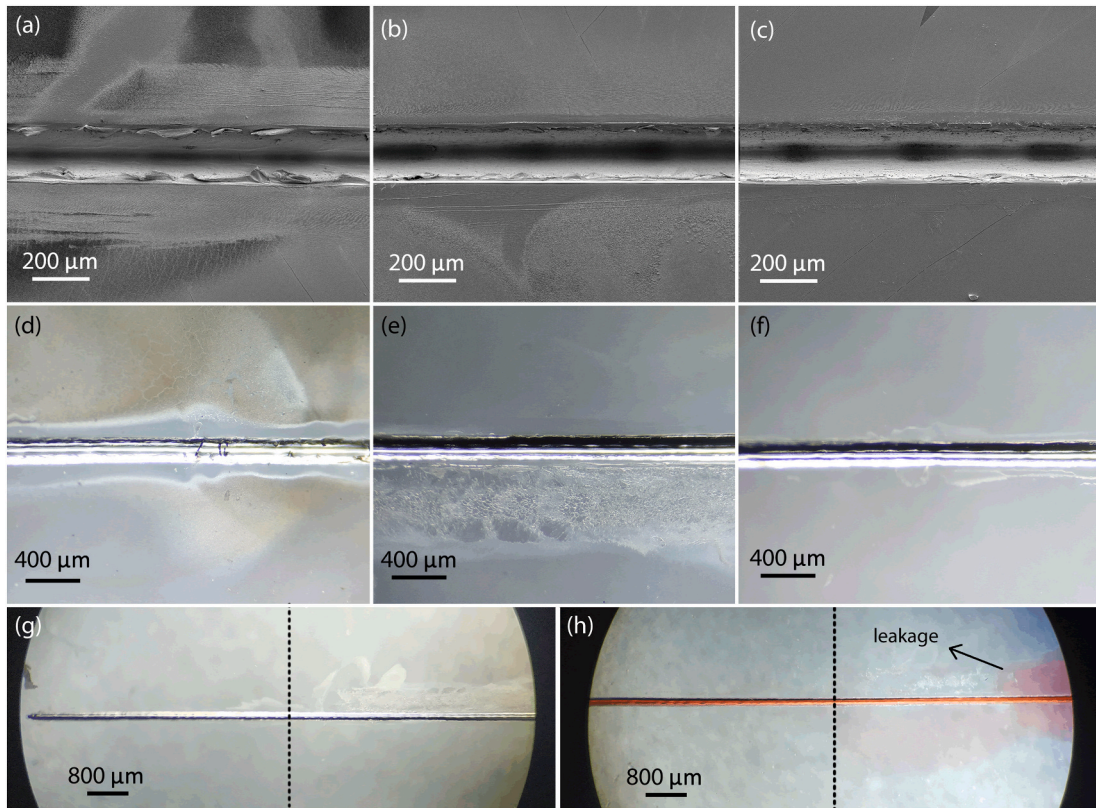


Fig. 5. Comparison of solvent and tape cleaned surfaces of PDMS slabs with their plasma bonding performances after laser machining. SEM image of PDMS slab a) immediately after laser machining the channel b) after cleaning with sonication in IPA and water bath for 5 min c) surface cleaned with the tape following the solvent cleaning process, the optical microscope image of the PDMS slab d) immediately after laser machining the channel e) after cleaning with sonication in IPA and water bath for 5 min f) following the solvent cleaning process the tape cleaned PDMS surface, the optical microscope image of tape cleaning (left side) and only solvent cleaning (right side) g) laser machined PDMS surface h) plasma bonded microchannel filled with red food dye dissolved in DI water that shows the right side with leakage due to the ashes that remained on the PDMS surface and which blocked plasma bonding to the glass substrate. (For interpretation of the references to color in this figure legend, the reader is referred to the web version of this article.)

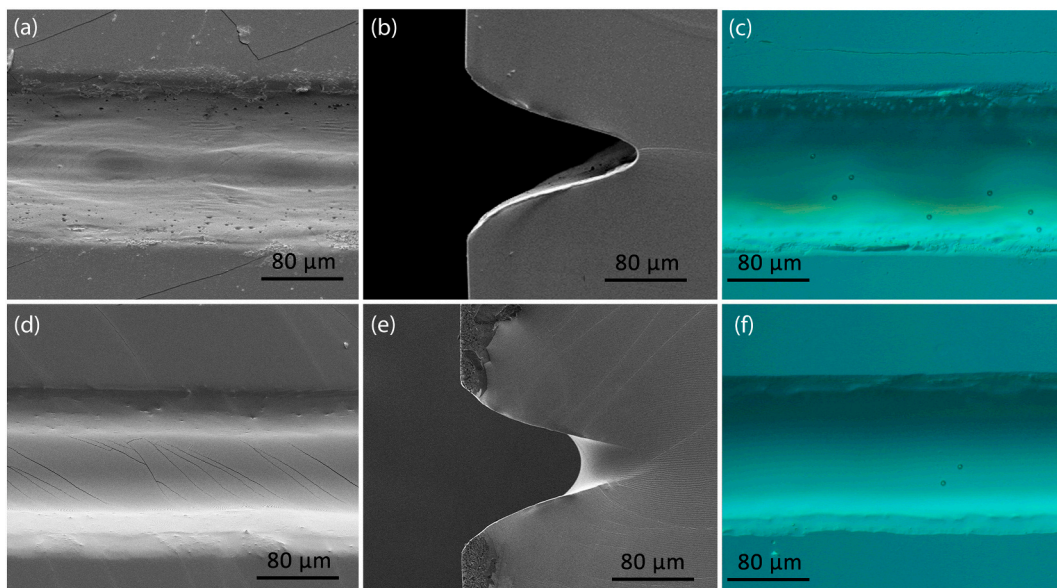


Fig. 6. Comparison of laser machined channel surface before and after PDMS spin coating. PDMS spin coated SEM images of a) channel surface b) cross section c) inverted microscope image of channel filled with 6 μm diameter PS beads suspended in DI water SEM image of channel after PDMS spin coating from d) top perspective e) cross section f) inverted microscope image of the channel after PDMS spin coating filled with 6 μm diameter PS beads suspended in DI water. Here the channel machining was carried out at 40% power, 100% speed and 5 kHz frequency settings.

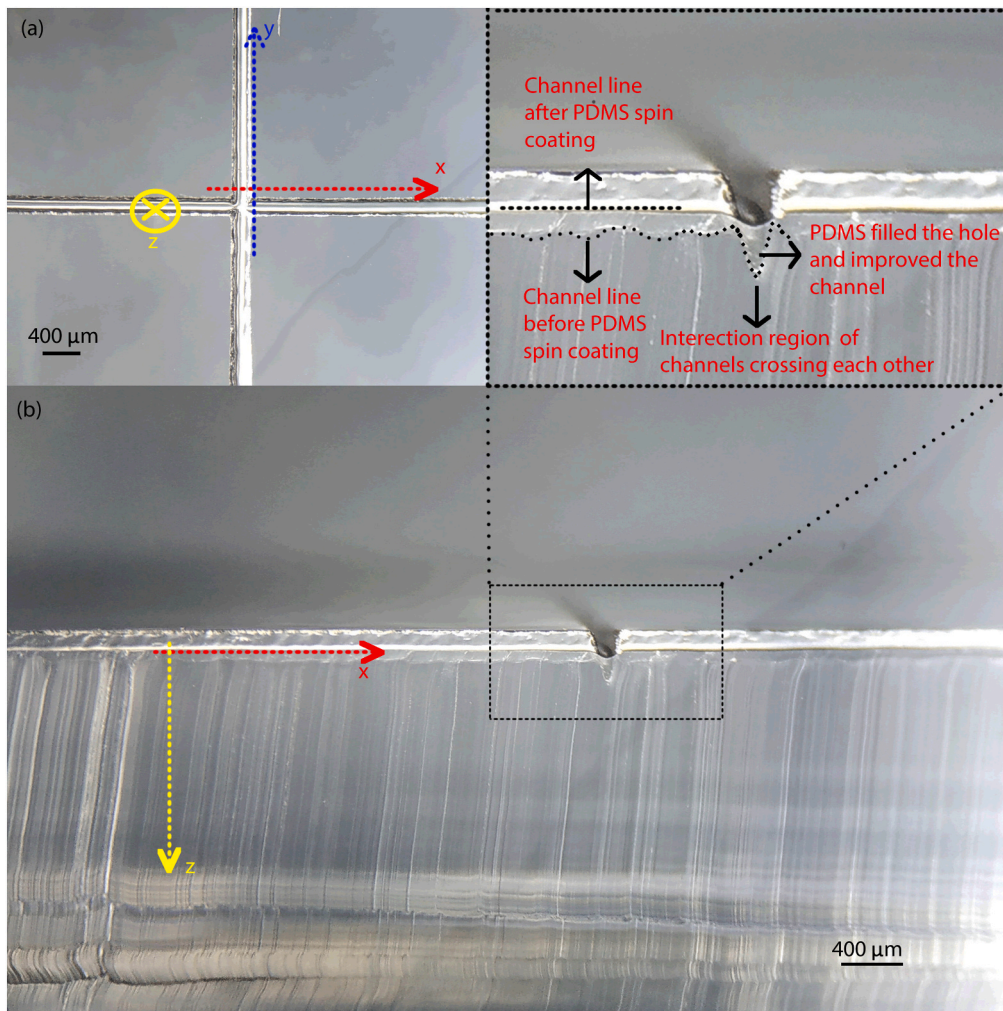


Fig. 7. Improvement of channel structure via PDMS spin coating. a) Optical microscope image of laser machined channels crossing each other from top view. b) Optical microscope image of cross section along the channel. The channels were engraved at 40% power, 100% speed and 5 kHz frequency settings.

exact focal point of the laser to achieve the highest possible intensity in the laser beam on the smallest area and ensure the maximum cutting performance. As the concern of this study was to carve microchannels rather than cutting, defocusing can be used as an additional parameter to tune the aspect ratio of the channel geometry. Elevating the working piece towards the focal lens brought the PDMS to a defocused area of the laser beam. Some previous works present engraving of channels on thermoplastic using a defocused laser beam [38]. Machining of the PDMS with a defocused laser beam gave similar results to the thermoplastic materials in terms of dimensions, where the enlarged beam, due to defocusing, induced wider and lower channels. The defocusing feature enabled increasing lateral channel dimensions in contrast to focused machining. Since the pulsed laser ablation mainly goes vertically down through the working piece, which makes ablation limited in the horizontal direction, it is significant when tuning channel dimensions in the horizontal aspect. The measurements of channel size at a defocused range between 1.5 and 6 mm for the two different regimes is given in Fig. 5S. Also, Fig. 4(a to d) illustrates the variation of channel dimension as well as surface smoothness of the channels across the defocused range with SEM images.

Fig. 4 shows SEM pictures of channels machined with a defocused laser beam at 5 kHz, 100% speed, and 60% power settings. The effect of the defocused laser beam on channel geometry was investigated by lifting up the working piece towards the focal lens in 1.5 mm steps. Results showed that the aspect ratio of the channel can be tuned by

arranging the distance between the working piece and the focusing lens. Fig. 6s also shows the calculated flow profile inside these channels given in Fig. 4.

3.3. The effect of cleaning on plasma bonding quality

Ablated material resolidifies over the PDMS surface during the laser machining of the channels. Therefore, some remnants are present both inside the channels and over the surface of the PDMS slab, as shown in Fig. 5(a) and (d). That debris need to be removed for two reasons: to facilitate plasma bonding between the machined PDMS and substrate, and to prevent channel clogging. So far, the main obstacle in making microfluidic chips from CO₂ laser machined PDMS has been the plasma bonding, which is impossible due to the modified surface morphology and chemistry of the PDMS after laser machining. None of the conventional cleaning methods adopted in microfluidic labs, which are air flux, water flush, rotary brush or sonication with solvents, can remove the debris over the PDMS surface, as shown in Fig. 5(b) and (e). As a result of inadequate cleaning of the PDMS surface, bonding fails and that leads to leakage during fluid flow through the channel as shown in Fig. 5(h). Failure to remove the ashes and debris from the PDMS surface has been the main reason for employing different materials instead of PDMS to create microfluidic chips through direct laser machining.

A practical way that enables the removal of ashes and debris remaining after laser ablation involves the use of tape to provide a clean

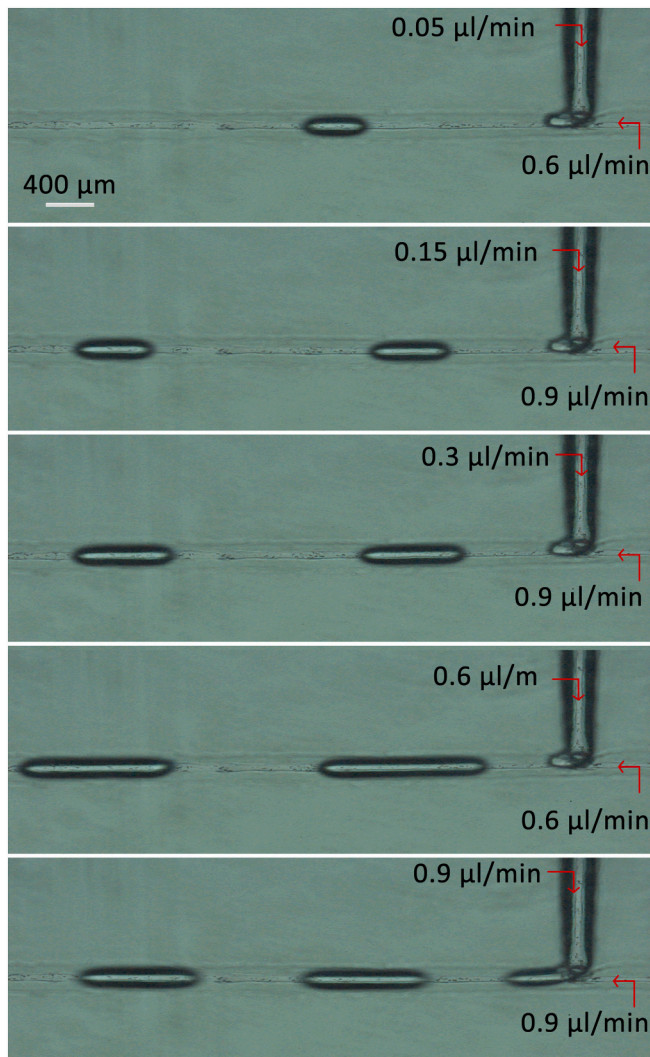


Fig. 8. Water in oil droplet generation in the laser machined T-junction.

surface that enables perfect plasma bonding. By attaching and detaching a tape several times using a fresh part of the strip each time, all the remnants covering the PDMS surface can be removed. Fig. 5(c) and (f) shows optical microscope images of the PDMS surface after tape cleaning. A direct comparison of tape-cleaned and solvent-cleaned sides of the same chip show the difference between the both methods more clearly. As shown on the left side of Fig. 5(g, h) the tape-cleaned side is pretty clear and well sealed through plasma bonding, while the right side is not so clean of ashes and not well sealed, giving rise to leakages. Testing the sealing achieved by tape cleaning and the resulting plasma bonded microfluidic chips was done by successfully pumping water through the channels at 2 bar (the limit of the pressure pump) for 1 h. When only solvent sonication cleaning was used, the start of leakage from the plasma bonded microfluidic chip was only a matter of time.

One should note that tape cleaning is necessary for plasma bonding although ultrasonic cleaning is not. However, during the flow experiment, furthermore ultrasonic cleaned microfluidic chips show better performance against clogging. Tape cleaning's inadequacy of reaching the channel interior while ultrasonic cleaning explains the fact very well. Therefore, it is recommended to apply solvent cleaning before or after the tape cleaning to have better flow performance.

3.4. Enhancement of channel surface quality

The laser ablation leaves a rough surface that is unfavorable for optical operations of the microfluidic chips. Particle detection via light scattering [39], cell deformability measurement [40], and imaging flow cytometry [41] are some of the applications of microfluidic chips that require good optical transparency. To improve surface roughness of the laser-engraved channels, a spin coating technique was applied that puts an extra uncured PDMS layer over the channels. Fig. 6(a) and (d) clearly shows the contrast between the PDMS spin coated and non-treated laser-engraved surfaces. The PDMS spin coating dramatically improved the surface roughness as well as reducing the curvature of the channel top forming a flatter top that is shown in Fig. 6(b) and (e). The thickness of the spin-coated PDMS layer is nonuniform and varies depending on the curvature. It can be up to 80 μm in the channel deep, 8–15 μm over the channel walls, and 20 μm on a flat surface at 2000 rpm, which can be further attenuated with upraising speed [42]. The optical performance of this pre-treatment was observed under an inverted microscope as

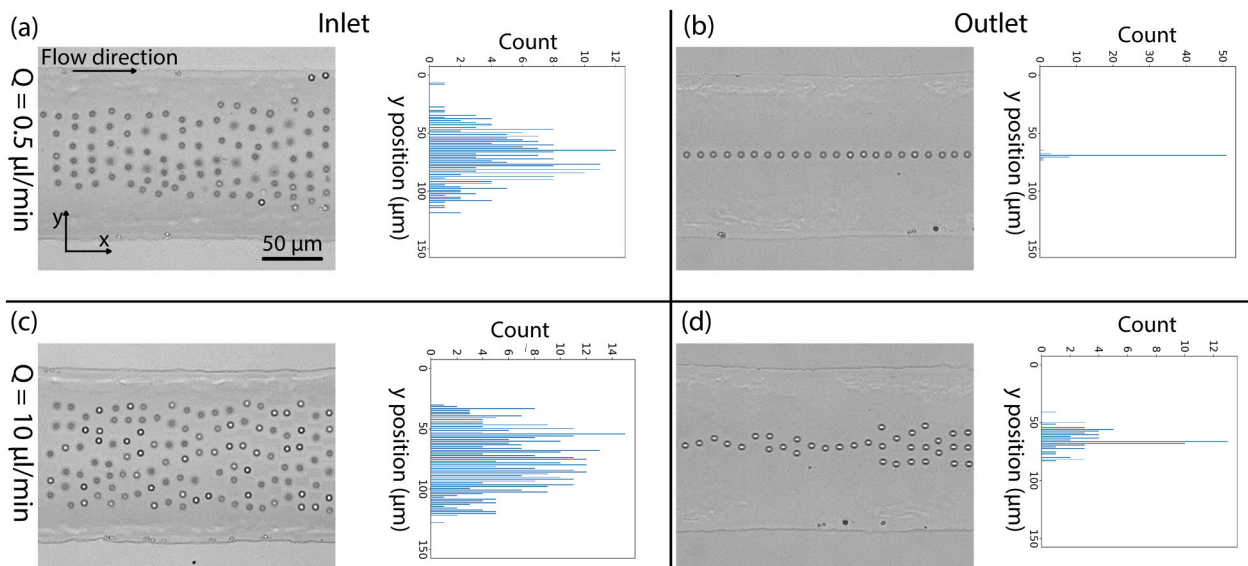


Fig. 9. Viscoelastic focusing of 6 μm diameter PS particles in straight microchannels are shown with stacked images and histograms. a) Inlet at 0.5 μl/min flow rate shows beads randomly distributed along the lateral axis b) outlet at 0.5 μl/min shows beads aligned into the middle of the channel by elastic lift force c) inlet at 10 μl/min shows beads randomly distributed along the lateral axis d) outlet at 10 μl/min shows distorted focusing due to inertial effects overcoming the elastic lift force.

shown in Fig. 6(c) and (f). According to this figure, PS bead inside the channel has clearer view, which enables better monitoring of the particles flowing through the channel.

The surface finish quality of the laser machining depends on the parameters like speed, power, and frequency. In the lowest power and the highest frequency and speed settings, the surface roughness is the lowest; towards the other end of these settings, surface roughness gets worse. Although PDMS spin coating is not mandatory especially for the channels fabricated with a good surface finish, it is recommended for improving the surface roughness since it is in favor of better flow and optical monitoring performance.

3.5. Smoothing the channel height variation

Depending on the processing parameters and design, the intersection domains of the channels crossing each other become bigger than the rest due to double ablation. Spin-coated PDMS fills these hollows elevating those deeper areas towards approximate general channel level. Yet it is not possible to totally align too deep and shallow areas, as PDMS is spin-coated on both areas. It also works to smooth the wavy and indented channel top that is inherited from the laser ablation associated with the processing parameters, and independent from the design. Fig. 7(a) shows a design consisting of two channels crossing each other. Fig. 7(b) shows the old indented tops and the new straight channel tops, as well as the old hollows at the intersection points of the channel, which is then filled by the spin coated PDMS.

Indentations at the channel top arising from the pulsed character of the laser have been flattened with the spin coated PDMS layer. As seen in this figure, the hollows or enlarged spaces in the intersections of the channels have been dramatically improved by the PDMS spin coating.

3.6. Applications

The performance of the direct laser machined microchannels in generating droplets and focusing viscoelastic microparticles showed great potential for further applications. Microfluidic chips fabricated in 10 min achieved the tasks very well, as discussed below:

3.6.1. Droplet generator

Droplet-based systems are one of the most fundamental topics in microfluidics, and they have been implemented in several fields, including particle synthesis [43] and detection [44]. Droplet generator incubator microchannels were manufactured using the 5 kHz, 50% speed and 30% power settings. As nanoliter droplets are among the most commonly used ones in microfluidic, the channel dimensions are specially designed to easily generate this size. Fig. 8 shows nanoliter droplet generation performance at the T junction of the channels. By arranging the flow rates of the water and oil, the frequency and size of the droplets are tuned as shown in the figure below. The inverted microscope images show that the droplet size and frequency can be finely tuned by regulating the flow rates of water and oil. The figure shows that the ratio of the flow rates between the oil and water determines how much volume the water will occupy along the channel. On the other hand, the total flow rate arranges the frequency of the droplet as well as its speed throughout the channel. Those parameters are significant with regards to sample volume and sampling speed where the sample is carried out inside the water droplets.

3.6.2. Viscoelastic focusing

Viscoelastic focusing of particles has recently gained popularity in microfluidic community addressing a significant issue such as the separation [45] or detection [46,47] of particles through aligning them on a single stream without using any other technique. A 5 cm-long microchannel with a width of 145 μm and a height of 70 μm was machined at 17% power, 100% speed and a frequency of 5 kHz. 6 micrometer diameter PS microbeads were suspended in an HA solution and sent to

the channel through a syringe pump at several flow rates. Randomly distributed beads in the entrance were focused into the middle of the channel by elastic force, which is dominant up to a flow rate of 5 $\mu\text{l}/\text{min}$, while advancing along the channel. Videos S1 and S2 show the dynamic plot of the high-speed camera outputs from the outlet of the microchannel at 0.5 $\mu\text{l}/\text{min}$ and 10 $\mu\text{l}/\text{min}$ respectively. At higher flow rates, the inertial lift force overcomes the elastic force and particle focusing decays [48]. Fig. 9(a, b) shows the channel inlet and outlet at 0.5 and 10 $\mu\text{l}/\text{min}$ flow rates via stacked images achieved by the particle trains. Aligning the particles into the middle favors not only the detection or sensing application, but also enables sample purification and enhancement thorough separation. All these bonus features come thanks to straight narrow channel geometry and a fluidic property without employing any external parts.

4. Conclusions

The fastest method for fabrication of PDMS microfluidic chips is via direct laser machining, which is the only method for engraving bulk PDMS that provides a design to plasma bond fabrication in 10 min. The only obstacle in making a plasma bonded microfluidic chip through direct laser machining was the debris left on the surface formed by the laser machining process. These remnants were effectively removed using a tape that could not have been achieved with other known techniques. The highest frequency and speed with the lowest power settings provided the best channel features. As the channel height and width is directly proportional to power, the laser machined channels lose interior smoothness as the dimensions increase. A simple pre-treatment method – PDMS spin coating of the laser machined channel – was shown to be effective in smoothing out the channel interior surface, which also decreased the aspect ratio of the channel. Defocusing the laser beam onto the working piece also means that the aspect ratio arrangement can be used as an additional machining parameter. The fabricated microfluidic chips showed high accuracy in droplet generation and viscoelastic particle focusing applications. With 1000 dpi resolution and down to a possible 32/12 μm height/width minimum channel size, this method offers high precision at a very low cost.

Supplementary data to this article can be found online at <https://doi.org/10.1016/j.jmapro.2021.11.016>.

Declaration of competing interest

The authors declare that they have no known competing financial interests or personal relationships that could have appeared to influence the work reported in this paper.

Acknowledgement

This study was financially supported by Kirikkale University BAP project no 2021/024. The author thanks to Prof. Caglar Elbuken for kind permission to use his laboratory; the author also thanks to Assist. Prof. Ismail Bilican for his help in SEM imaging. The author specially thanks to the great photograph artist Mete Ozdek, who passed away, for his help in arrangement of some figures.

References

- [1] Wang C-H, Lee G-B. Pneumatically driven peristaltic micropumps utilizing serpentine-shape channels. *J Micromech Microeng* 2006;16(2):341–8.
- [2] Guler MT, Beyazkılıç P, Elbuken C. A versatile plug microvalve for microfluidic applications. *Sens. Actuators, A* 2017;265:224–30.
- [3] Duffy DC, McDonald JC, Schueller OJ, Whitesides GM. Rapid prototyping of microfluidic systems in poly (dimethylsiloxane). *Anal Chem* 1998;70(23):4974–84.
- [4] Cosson S, Aeberli LG, Brandenberg N, Lutolf MP. Ultra-rapid prototyping of flexible, multi-layered microfluidic devices via razor writing. *Lab Chip* 2015;15(1): 72–6.

- [5] McDonald JC, Chabiny ML, Metallo SJ, Anderson JR, Stroock AD, Whitesides GM. Prototyping of microfluidic devices in poly (dimethylsiloxane) using solid-object printing. *Anal Chem* 2002;74(7):1537–45.
- [6] Xue B, Geng Y, Yan Y, Ma G, Wang D, He Y. Rapid prototyping of microfluidic chip with burr-free PMMA microchannel fabricated by revolving tip-based micro-cutting. *J Mater Process Technol* 2020;277:116468–82.
- [7] Trotta G, Volpe A, Ancona A, Fassi I. Flexible micro manufacturing platform for the fabrication of PMMA microfluidic devices. *J Manuf Process* 2018;35:107–17.
- [8] Bartholomeusz DA, Boutté RW, Andrade JD. Xurography: rapid prototyping of microstructures using a cutting plotter. *J Microelectromech Syst* 2005;14(6):1364–74.
- [9] Hwang Y, Seo D, Roy M, Han E, Candler RN, Seo S. Capillary flow in PDMS cylindrical microfluidic channel using 3-D printed mold. *J Microelectromech Syst* 2016;25(2):238–40.
- [10] Comina G, Suska A, Filippini D. PDMS lab-on-a-chip fabrication using 3D printed templates. *Lab Chip* 2014;14(2):424–30.
- [11] Juskova P, Ollitraul A, Serra M, Viovy J-L, Malaquin L. Resolution improvement of 3D stereo-lithography through the direct laser trajectory programming: application to microfluidic deterministic lateral displacement device. *Anal Chim Acta* 2018;1000:239–47.
- [12] Parker B, Samanipour R, Ahmadi A, Kim K. Rapid fabrication of circular channel microfluidic flow-focusing devices for hydrogel droplet generation. *Micro Nano Lett* 2016;11(1):41–5.
- [13] Carugo D, Lee JY, Pora A, Browning RJ, Capretto L, Nastruzzi C, Stride E. Facile and cost-effective production of microscale PDMS architectures using a combined micromilling-replica moulding (μ Mi-REM) technique. *Biomed Microdevices* 2016;18(1):4–14.
- [14] Serhatlioglu M, Elbuken C, Ortaç B, Solmaz ME. Femtosecond laser fabrication of fiber based optofluidic platform for flow cytometry applications. In: *Optical Fibers and Sensors for Medical Diagnostics and Treatment Applications XVII*. International Society for Optics and Photonics; 2017. 100580I-5.
- [15] Bellouard Y, Said A, Dugan M, Bado P. Fabrication of high-aspect ratio, microfluidic channels and tunnels using femtosecond laser pulses and chemical etching. *Opt Express* 2004;12(10):2120–9.
- [16] Borasi L, Casamenti E, Charvet R, Dénéreaz C, Pollonghini S, Deillon L, Yang T, Ebrahim F, Mortensen A, Bellouard Y. 3D metal freeform micromanufacturing. *J Manuf Process* 2021;68:867–76.
- [17] Said AA, Dugan M, Bado P, Bellouard Y, Scott A, Mabesa Jr JR. In: *Manufacturing by laser direct-write of three-dimensional devices containing optical and microfluidic networks*. International Society for Optics and Photonics; 2004. p. 194–204.
- [18] Serhatlioglu M, Ortaç B, Elbuken C, Biyikli N, Solmaz ME. CO₂ laser polishing of microfluidic channels fabricated by femtosecond laser assisted carving. *J Micromech Microeng* 2016;26(11):115011–20.
- [19] Kim TN, Campbell K, Groisman A, Kleinfeld D, Schaffer CB. Femtosecond laser-drilled capillary integrated into a microfluidic device. *Appl Phys Lett* 2005;86(20):201106–9.
- [20] Hsieh Y-K, Chen S-C, Huang W-L, Hsu K-P, Gorday KAV, Wang T, Wang J. Direct micromachining of microfluidic channels on biodegradable materials using laser ablation. *Polymers* 2017;9(7):242–58.
- [21] Isiksacan Z, Guler MT, Aydogdu B, Bilican I, Elbuken C. Rapid fabrication of microfluidic PDMS devices from reusable PDMS molds using laser ablation. *J Micromech Microeng* 2016;26(3):035008–16.
- [22] Prakash S, Kumar S. Pulse smearing and profile generation in CO₂ laser micromachining on PMMA via raster scanning. *J. Manuf. Process.* 2018;31:116–23.
- [23] Guler MT, Isiksacan Z, Serhatlioglu M, Elbuken C. Self-powered disposable prothrombin time measurement device with an integrated effervescent pump. *Sens Actuators B* 2018;273:350–7.
- [24] Hong T-F, Ju W-J, Wu M-C, Tai C-H, Tsai C-H, Fu L-M. Rapid prototyping of PMMA microfluidic chips utilizing a CO₂ laser. *Microfluid Nanofluid* 2010;9(6):1125–33.
- [25] Li H, Fan Y, Kodzius R, Foulds IG. Fabrication of polystyrene microfluidic devices using a pulsed CO₂ laser system. *Microsyst Technol* 2012;18(3):373–9.
- [26] Yap YC, Guijt RM, Dickson TC, King AE, Breadmore MC. Stainless steel pinholes for fast fabrication of high-performance microchip electrophoresis devices by CO₂ laser ablation. *Anal Chem* 2013;85(21):10051–6.
- [27] Bilican I, Guler MT. Assessment of PMMA and polystyrene based microfluidic chips fabricated using CO₂ laser machining. *Appl Surf Sci* 2020;534:147642–51.
- [28] Chen X, Shen J, Zhou M. Rapid fabrication of a four-layer PMMA-based microfluidic chip using CO₂-laser micromachining and thermal bonding. *J Micromech Microeng* 2016;26(10):107001–8.
- [29] Guler MT, Inal M, Bilican I. CO₂ laser machining for microfluidics mold fabrication from PMMA with applications on viscoelastic focusing, electrospun nanofiber production, and droplet generation. *J Ind Eng Chem* 2021;98:340–9.
- [30] Chan SH, Nguyen N-T, Xia Z, Wu Z. Development of a polymeric micro fuel cell containing laser-micromachined flow channels. *J Micromech Microeng* 2004;15(1):231–6.
- [31] Liu H-B, Gong H-Q. Templateless prototyping of polydimethylsiloxane microfluidic structures using a pulsed CO₂ laser. *J Micromech Microeng* 2009;19(3):037002–10.
- [32] Holle AW, Chao S-H, Holl MR, Houkal JM, Meldrum DR. Characterization of program controlled CO₂ laser-cut PDMS channels for lab-on-a-chip applications. In: *2007 IEEE International Conference on Automation Science and Engineering*; 2007. p. 621–7.
- [33] Fogarty BA, Heppert KE, Cory TJ, Hulbutta KR, Martin RS, Lunte SM. Rapid fabrication of poly (dimethylsiloxane)-based microchip capillary electrophoresis devices using CO₂ laser ablation. *Analyst* 2005;130(6):924–30.
- [34] Yuen MC, Kramer RK. Fabricating microchannels in elastomer substrates for stretchable electronics, international manufacturing science and engineering conference. *American Society of Mechanical Engineers* 2016:1–9.
- [35] Guler MT, Bilican I. Capacitive detection of single bacterium from drinking water with a detailed investigation of electrical flow cytometry. *Sens. Actuators, A* 2018;269:454–63.
- [36] Kumar R. A review on RF micro-electro-mechanical-systems (MEMS) switch for radio frequency applications. *Microsyst. Technol.* 2020:1–18.
- [37] Guler MT. Definition and detection of simulation noise via imaginary simulated particles in comparison with an electrical microfluidic chip noise. *Microsyst. Technol.* 2021;27(5):2075–89.
- [38] Romoli L, Tantussi G, Dini G. Experimental approach to the laser machining of PMMA substrates for the fabrication of microfluidic devices. *Opt Lasers Eng* 2011;49(3):419–27.
- [39] Zhuang G, Jensen TG, Kutter JP. Detection of unlabeled particles in the low micrometer size range using light scattering and hydrodynamic 3D focusing in a microfluidic system. *Electrophoresis* 2012;33(12):1715–22.
- [40] Youn S, Lee DW, Cho Y-H. Cell-deformability-monitoring chips based on strain-dependent cell-lysis rates. *J Microelectromech Syst* 2008;17(2):302–8.
- [41] Zhu H, Mavandadi S, Coskun AF, Yaglidere O, Ozcan A. Optofluidic fluorescent imaging cytometry on a cell phone. *Anal Chem* 2011;83(17):6641–7.
- [42] Isgor PK, Marcali M, Keser M, Elbuken C. Microfluidic droplet content detection using integrated capacitive sensors. *Sens Actuators B* 2015;210:669–75.
- [43] Saateh A, Kalantarifard A, Celik OT, Asghari M, Serhatlioglu M, Elbuken C. Real-time impedimetric droplet measurement (iDM). *Lab Chip* 2019;19(22):3815–24.
- [44] Kalantarifard A, Saateh A, Elbuken C. Label-free sensing in microdroplet-based microfluidic systems. *Chemosensors* 2018;6(2):23–51.
- [45] Asghari M, Cao X, Mateescu B, Van Leeuwen D, Aslan MK, Stavrakis S, deMello AJ. Oscillatory viscoelastic microfluidics for efficient focusing and separation of nanoscale species. *ACS Nano* 2019;14(1):422–33.
- [46] Serhatlioglu M, Asghari M, Tahsin Guler M, Elbuken C. Impedance-based viscoelastic flow cytometry. *Electrophoresis* 2019;40(6):906–13.
- [47] Asghari M, Serhatlioglu M, Ortaç B, Solmaz ME, Elbuken C. Sheathless microflow cytometry using viscoelastic fluids. *Sci Rep* 2017;7(1):1–14.
- [48] Lu X, Liu C, Hu G, Xuan X. Particle manipulations in non-newtonian microfluidics: a review. *J Colloid Interface Sci* 2017;500:182–201.